


## Design and development status of the ITER Radial Gamma Ray Spectrometer<sup>☆</sup>

Federico Scioscioli <sup>a,b</sup> <sup>\*</sup>, Giulia Marcer <sup>a,b</sup>, Alessandro Ciurlino <sup>a</sup>, Stefano Colombi <sup>a</sup>, Bruno Coriton <sup>c</sup>, Andrea Dal Molin <sup>b</sup>, Jan Dankowski <sup>c,d</sup>, Giuseppe Gorini <sup>a,b</sup>, Andrei Kovalev <sup>c</sup>, Andrea Muraro <sup>b</sup>, Massimo Nocente <sup>a</sup>, Marica Rebai <sup>b</sup>, Davide Rigamonti <sup>b</sup>, Marco Tardocchi <sup>b</sup>, Gabriele Croci <sup>a,b</sup>

<sup>a</sup> University of Milano-Bicocca, Piazza della Scienza 3, Milan, 20126, Italy

<sup>b</sup> Institute for Plasma Science and Technology, National Research Council, Via R. Cozzi 53, Milan, 20125, Italy

<sup>c</sup> ITER Organization, Route de Vinon-sur-Verdon - CS 90 046, St. Paul-lez-Durance, 13067, France

<sup>d</sup> Institute of Nuclear Physics, Walerego Eliasza Radzikowskiego 152, Krakow, 31342, Poland

### ARTICLE INFO

#### Keywords:

ITER diagnostics  
Gamma-ray spectrometry  
Radial gamma ray spectrometer  
Fast ions  
Runaway electrons  
Fusion power

### ABSTRACT

The ITER Radial Gamma Ray Spectrometer (RGRS) is an ITER diagnostic located in the Equatorial Port 01 undergoing its Preliminary Design Review and foreseen for Phase DT1 (2041). RGRS is expected to measure the density profile and energy distribution of  $\alpha$ -particles through reactions with  $^{10}\text{B}$ , the current and maximum energy of runaway electrons through bremsstrahlung emissions, and fusion power via a radiative channel of the DT reaction. The diagnostic employs  $\text{LaBr}_3$  scintillators coupled with PMTs along 4 radial lines of sight, with LiH attenuators to reduce the background due to direct neutrons and a heavily hydrogenated and borated concrete-like mixture for neutron shielding.

Performance assessments indicate RGRS can fulfil its functions regarding runaway electrons, while the feasibility of measuring  $\alpha$ -particles is uncertain due to the intense gamma-ray background observed at JET. Further study is needed to confirm this measurement possibility. Additionally, while fusion power measurements appear possible, satisfying ITER requirements necessitates detailed knowledge of the gamma-ray-to-neutron branching-ratio of the DT reaction, which will be investigated through dedicated experiments, and possibly gamma-ray attenuators to reduce background.

### 1. Introduction

The primary aims of gamma-ray measurements in the several MeV range at ITER are threefold: (i) to measure the profile and energy distribution of  $\alpha$ -particles born from DT reactions, (ii) to detect and study runaway electrons (REs) generated during disruptions, and (iii) to provide a neutron-independent fusion power measurement.

For  $\alpha$ -particle studies, gamma-rays emitted by confined fast ions, including  $\alpha$ -particles, reacting with impurities can be utilized to probe their energy distribution and spatial profile [1]. Following the ITER rebaselining, the most important impurity in this regard appears to be  $^{10}\text{B}$ , which emits gamma-rays in the 3 to 4 MeV range [2]. Analysis of the intensity and shape of the associated full-energy peaks in the

observed Pulse Height Spectrum (PHS) allows to investigate the energy distribution of fast ions. For RE studies, focus is placed on thin-target bremsstrahlung, i.e. confined REs interacting with the bulk plasma, which generates a continuous energy spectrum. The broadband shape of this spectrum is relevant, rather than a narrow energy band [3,4]. Finally, the radiative channel of the DT fusion reaction emits gamma-rays over a wide spectral region around 15 MeV, enabling the determination of the neutron yield, and hence of the fusion power, from the absolute counting of the emitted high-energy gamma-rays [5,6].

This paper presents the design of the Radial Gamma-Ray Spectrometer (RGRS) for ITER. This is a diagnostic system currently in its Preliminary Design Review (PDR) phase and foreseen by the ITER

<sup>☆</sup> The following acronyms are used throughout the paper: BP (Bioshield Plug); DT (Deuterium-Tritium); EQ01 (ITER Equatorial Port 01); HRNS (High Resolution Neutron Spectrometer); LoS (Line of Sight); Monte Carlo (MC); PC (Port Cell); PCA (Principal Component Analysis); PDR (Preliminary Design Review); PMT (Photo-Multiplier Tube); RE (Runaway Electron); RGRS (Radial Gamma Ray Spectrometer); RNC (Radial Neutron Camera); SiPM (Silicon Photomultiplier); ToF (Time-of-Flight).

<sup>\*</sup> Corresponding author at: University of Milano-Bicocca, Piazza della Scienza 3, Milan, 20126, Italy.

E-mail address: [federico.scioscioli@unimib.it](mailto:federico.scioscioli@unimib.it) (F. Scioscioli).

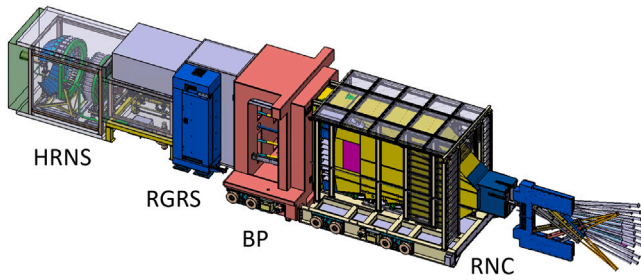


Fig. 1. View of the components of the Equatorial Port 01 of greatest importance for RGRS: the Radial Neutron Camera (RNC); the Bioshield Plug (BP); RGRS itself; and the High-Resolution Neutron Spectrometer (HRNS).

baseline for phase DT1 (2041). The design is based on past experience with gamma-ray measurements at the JET tokamak, but also benefits from the plurality of Lines of Sight (LoSs) available at ITER. After an overview of the system, the main technical challenge with gamma-ray spectrometry on large tokamaks - background - is addressed. Finally, the performances of RGRS in fulfilling the three above-mentioned requirements are assessed.

## 2. RGRS overview and layout

RGRS is located in the Port Cell (PC) of the Equatorial Port 01 (EQ01) of the ITER tokamak, behind the Radial Neutron Camera (RNC) [7] and the Bioshield Plug (BP) and in front of the High-Resolution Neutron Spectrometer (HRNS) [8]. RGRS lies at about 18 m from the tokamak centre and operates at room temperature. A view of the relevant systems is shown in Fig. 1.

### 2.1. Generalities

RGRS views the plasma through four radial LoSs. Three of these LoSs are coplanar and dedicated to RGRS, while the fourth lies in a different plane and is shared with RNC. All four LoSs are cylindrical in shape, with the dedicated ones having a diameter of 40 mm and the shared one measuring 25 mm. The system is also crossed along its entire radial extension by a LoS dedicated to HRNS, with diameter 41 mm.

As shown in Fig. 2, most of the RGRS volume is filled with a concrete-like mixture, as detailed in Section 3.2. The detectors are accessible from the left side, facing the tokamak, through openings in the concrete that are filled with concrete bricks during operation.

To facilitate insertion and removal of the detectors, a simple manually-activated rail system is present. As the system is located downstream of the BP, shutdown dose-rates are sufficiently low to allow human access after a few days of cooling. Therefore, detector replacement in case of failure can be carried out by human personnel during long-term maintenance without any remote handling.

### 2.2. Detectors

Each LoS is equipped with a  $\text{LaBr}_3 : \text{Ce}$  scintillator coupled with a Photo-Multiplier Tube (PMT). This is the fastest commercially available inorganic scintillator, essential for sustaining the count-rates expected during full-power discharges - roughly in the range 500 kHz to 1 MHz. Similarly, PMTs with linear-dynode configurations are also required to handle these high count-rates. A large crystal volume of  $3 \text{ in} \times 3 \text{ in}$  is also necessary to fully stop gamma-rays for accurate fusion power measurement.

The gain of a PMT is highly sensitive to magnetic fields. Although electromagnetic transients are not expected to be a concern at the radial position of RGRS, the magnetostatic field is estimated to be 142 mT perpendicular to the PMT axis and 33 mT parallel to it. Given that PMTs

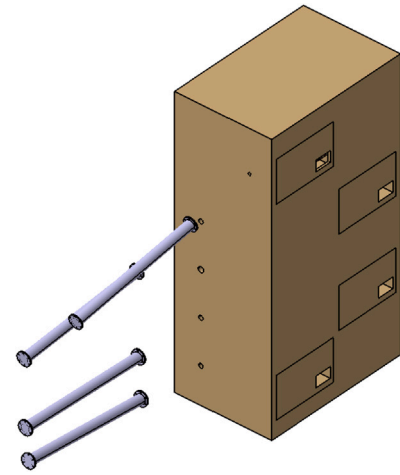


Fig. 2. Computer model of RGRS. The grey cylinder contain the LiH attenuators, while the tan body is the concrete-like filling material.

Table 1

Materials and radii (inner and outer) of the magnetic shield. All layers are 450 mm long and open on both ends. The total mass is about 76 kg.

Material	$r_i$ (mm)	$r_o$ (mm)
Hiperco 50A	51	71
Mu-metal	72	74
Mu-metal	75	77
Hiperco 50A	78	98

equipped with linear dynodes require fields not exceeding  $20 \mu\text{T}$  and  $100 \mu\text{T}$  in these directions, magnetic shielding is necessary. Incidentally, the large detector area precludes replacing PMTs with SiPMs.

The shielding design is detailed in Table 1. It consists of four concentric cylindrical layers: the innermost and outermost are made of Hiperco 50 A [9], a high-permeability Fe-Co-V soft magnetic alloy, while the two central layers are in mu-metal. The use of a soft material in the innermost layer is necessary to shield against fields parallel to the shield axis. The presence of Co, which is subject to intense neutron activation, is not expected to be an issue due to its shielded location.

The preamplifiers necessary to operate the detectors are located in a shielded cabinet shared with RNC and adjacent to RGRS. Both the raw and preamplified signals are acquired. The digitizers and later stages in the electronic chain are in an external building.

## 3. Background sources

The RGRS scintillators are sensitive not only to gamma-rays, but also to fast neutrons. In fact, the overall efficiency of large  $\text{LaBr}_3$  crystals to 14 MeV neutrons is higher than to gamma-rays [10]. RGRS is therefore subject to background due to several sources.

### 3.1. Direct neutrons

At the RGRS location, neutrons streaming along the LoSs are expected to overwhelm the gamma-ray signal by about 5 orders of magnitude. This being unacceptable, some attenuator is required. This attenuator should be selective, i.e., essentially transparent to MeV-range gamma-rays, while absorbing neutrons.

Several materials were considered, the final choice being LiH. This is the same material already adopted for gamma-spectrometry at JET [11,12]. Compared with other options, notably B-based absorbers, it presents low gamma-ray emissions. It can be manufactured in pressed pellets up to about 93% of the theoretical density, which is  $0.78 \text{ g cm}^{-3}$ .

As shown in Fig. 3, an attenuator 1.2 m long is appropriate for the ITER purposes, enabling to re-establish the signal-to-noise ratio to

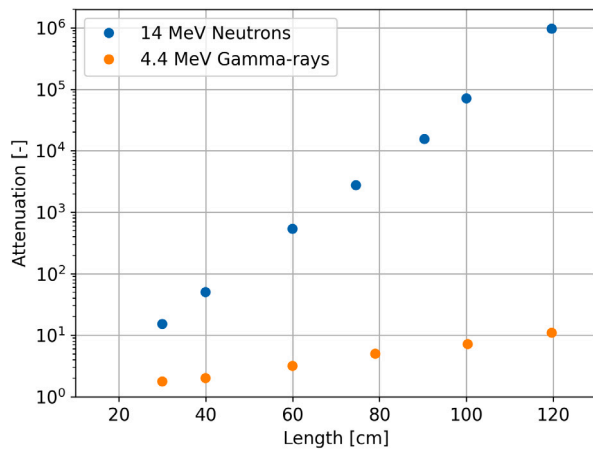


Fig. 3. Attenuation factor for 14 MeV neutrons and 4.44 MeV gamma-rays as a function of the LiH attenuator length. The gamma-ray energy, corresponding to the first  $^{12}\text{C}$  excited state, is chosen as representative of the direct gamma-rays background, lying around the spectrum mid-point. All values were found through Monte Carlo simulations of the isolated attenuator.

acceptable values. The attenuators, one per LoS, are placed through the BP inside concrete-filled metal cassettes. LiH being a hazardous material, subject to violent reactions with both air and water, the pellets are piled and encapsulated within a 316LN stainless steel tube. Analyses are ongoing to assess gaseous swelling and tritium production inside the pellets, though experience at JET and unpublished calculations for the ITER Neutral Particle Analyser [13], which also uses LiH at a similar distance from the tokamak, suggest full compatibility with the safety requirements.

### 3.2. Scattered neutrons

As discussed in Section 2, RGRS is crossed by a LoS along its whole radial extension. This LoS being devoted to a neutron diagnostic, the neutron flux along it reaches  $1 \times 10^9 \text{ n cm}^{-2} \text{ s}^{-1}$  during full-power discharges. Rough estimates show that if the inside volume of RGRS were empty, scattering by air alone would generate count-rates in the hundreds kHz range at the detectors closest to the LoS. This is the primary reason to fill the RGRS volume with a neutron shield.

The chosen material is SWX-277Z-5, a heavily hydrogenated (4.73 wt %) and borated (4.99 wt %) concrete-like mixture [14]. Due to its refractory properties, this material maintains physical integrity up to 1038 °C, which is sufficient for the worst fire conditions anticipated for the PC (820 °C). Moreover, it is also castable, allowing to manufacture the LoSs by positioning flight tubes during casting instead of drilling.

Preliminary MC simulations of the whole EQ01 show that the full-power neutron flux at the detector positions ranges from  $1 \times 10^4$  to  $8 \times 10^4 \text{ n cm}^{-2} \text{ s}^{-1}$  depending on the detector. While high, these fluxes are manageable thanks to the choice of  $\text{LaBr}_3$  as scintillation material.

### 3.3. Direct gamma-rays

Experience at JET shows the presence of an intense gamma-ray background up to about 10 MeV. This background is due to gamma-rays streaming along the LoS, so there is no way to suppress it without also reducing the signal.

The precise nature of this background is still being investigated, but it clearly consists of prompt gamma-rays emitted along the LoS by neutrons impinging on the LoS footprint on the vacuum vessel. Indeed, some features can be recognized in the PHS [5] of the JET Inconel vacuum vessel main constituents, Ni and Cr, and a Monte Carlo (MC) simulation focusing on these gamma-rays reproduces the experimental spectrum at least qualitatively.

This background is expected to heavily affect  $\alpha$ -particle measurements, which involve gamma-rays in this spectral region. However, the relevance of the observed JET spectra is unclear for ITER, given the different materials, size and structure for both first wall and vacuum vessel. It is instead clear that RE and fusion power measurements are not directly impacted: RE are associated with intensities high enough to overwhelm this background, while DT gamma-rays lie in a different spectral region. The only way these latter measurements can therefore be affected by this background is through pile-up. This is discussed further in Section 4.3.

### 3.4. Environmental gamma-rays

The RGRS scintillators need shielding against gamma-rays due to neutron interactions with the surrounding materials. These include both prompt emissions not along the LoS and activation gamma-rays.

Given that typical activation gamma-rays have relatively low energy and that the RGRS detectors are already inside a thick concrete-like shield, a relatively simple gamma-ray shield consisting of Pb bricks is found to be sufficient. Each detector has its own shield. In order to be compatible with fire conditions in the PC, which exceed the Pb melting temperature, bricks are steel-cladded. Accordingly, some care is required to avoid radiation leaking.

## 4. Performances

As discussed in the Introduction, RGRS has three objectives: (i) measuring the profile and energy distribution of  $\alpha$ -particles born from DT reactions, (ii) detecting and quantifying runaway electrons (REs) generated during disruptions, and (iii) providing a neutron-independent fusion power measurement.

### 4.1. $\alpha$ -particles

At the time RGRS underwent its first design, the ITER first wall was made of Be. Indeed, a similar ITER-like wall was installed at JET. Accordingly, both the first RGRS design and gamma-ray spectrometry at JET revolved around observing the  $^9\text{Be}(\alpha, n)^{12}\text{C}$  reaction through the de-excitation gamma-rays emitted by the  $^{12}\text{C}$  nucleus.

The new ITER baseline replaces the Be first wall with W. Therefore, Be is no longer present in the plasma as an impurity, so that the above reaction cannot be exploited. Accordingly, other reactions are being investigated.

#### 4.1.1. Noble gases

An investigation of reactions between  $\alpha$ -particles and noble gases requiring positive  $Q$ -value, or at least an energy threshold not too close to the DT fusion  $\alpha$ -particle kinetic energy of 3.5 MeV, and cross section at least in the several mb range provides as only candidates  $^{20}\text{Ne}(\alpha, \alpha)^{20}\text{Ne}^*$ , which emits at 1.63 MeV, in the region where  $\text{LaBr}_3$  exhibits intrinsic radioactivity, and  $^{22}\text{Ne}(\alpha, n)^{25}\text{Mg}$ , which however becomes significantly probable only for energies above 3 MeV. Thus, reactions with noble gases appear to be challenging.

#### 4.1.2. Boron

The most promising candidate is  $^{10}\text{B}$ , whose reactions with  $\alpha$ -particles release gamma-rays at three different energies: 3.09, 3.68 and 3.85 MeV. Fig. 4 shows the respective cross sections as functions of the  $\alpha$ -particle energy. All three lines are in principle exploitable.

Natural B is present in the ITER plasma as an impurity due to wall-conditioning, though at the moment neither its concentration nor its density profile are known. Here, a 1% B concentration is adopted with the same density profile as for electrons. This latter assumption is motivated by light impurities transport being dominated by turbulence [15]. The natural isotopic abundance of 19.9% is assumed for  $^{10}\text{B}$ .

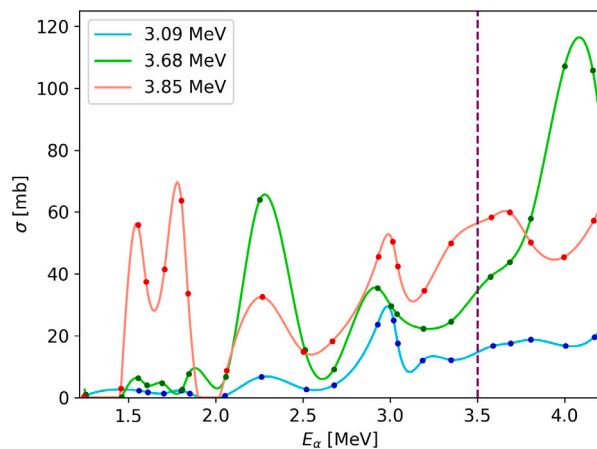


Fig. 4. Cross sections for B reactions as functions of  $\alpha$ -particle energy [2]. Experimental data points are presented alongside cubic interpolations. The dashed vertical line corresponds to the energy of DT fusion  $\alpha$ -particles.

As mentioned in Section 3.3, the main issue with  $\alpha$ -particle measurements is the direct gamma-ray background. This aspect is crucial in determining whether  $\alpha$ -particle measurements are feasible and with which performances. Currently MC simulations up to the tokamak central column are being set up, aiming to quantify this background for ITER to assess its effects on  $\alpha$ -particle measurements. It is however unclear how reliable prompt gamma-ray cross section data for high-energy neutrons are.

#### 4.2. Runaway electrons

The Conceptual Design considerations about REs previously published in [16] remain valid for the current design stage of RGRS. This paper therefore only provides a brief summary.

RGRS focuses on detecting thin-target bremsstrahlung, which involves the hard X-rays (HXRs) emitted when confined REs interact with the bulk plasma. This is in contrast to thick-target bremsstrahlung, where REs leave the plasma and interact with the tokamak structures. The interest lies in both the intensity of the RE beam and its energy distribution.

Since bremsstrahlung emits an energy continuum, the entire spectrum shape is relevant for RE studies. In particular, the RE distribution function and current can be obtained from the measured spectrum by a deconvolution method that accounts for both the HXR emission process and the detector response function. As the bremsstrahlung spectrum extends up to almost the RE energy, which can be as high as 100 MeV on ITER, the background of Section 3.3 is not a concern in most scenarios.

Given a typical disruption duration of 100 ms, achieving a time-resolved measurement requires working on a timescale of 10 ms. To ensure sufficient counts for the deconvolution algorithm to work properly, a RE current of at least 10 MA is necessary. However, if the time resolution requirement is relaxed and the disruption duration is integrated over, it becomes possible to measure RE currents down to 1 MA. These values apply to an unmitigated scenario. The use of gas injection as a mitigation technique would enhance bremsstrahlung emissions due to the addition of heavy neutral scatterers in the plasma, enabling measurement of RE currents as low as 40 kA, even in a time-resolved mode.

It should be mentioned that the probability for a RE to produce a HXR along the radial direction decreases with increasing energy, due to the emission becoming more forward. Consequently, the sensitivity of RGRS is limited to detecting RE energy distributions up to approximately 30–40 MeV.

#### 4.3. Fusion power

Fusion power measurement with RGRS relies on detecting de-excitation gamma-rays from the  $D + T \rightarrow {}^5\text{He}^*$  reaction. Two such gamma-rays exist, with nominal energies at 12.5 and 16.75 MeV; they exhibit significant intrinsic broadening [5]. By counting gamma-rays in this spectral region and having established suitable transport coefficients through simulations, it is possible to determine the LoS-integrated fusion gamma-ray emissivity, and hence the neutron rate and fusion power. This technique was tested at JET as part of the GET-ART project [6].

The transport coefficients mentioned above depend on the plasma scenario through the plasma position and shape. Consequently, it is not possible for a single gamma-ray detector to distinguish between variations in fusion power and changes in the plasma scenario as causes of fluctuations in count-rates. This limitation necessitates the use of several LoSs for RGRS: even without full tomographic reconstruction, looking at the plasma through different LoSs allows compensating for variations in one detector with those in another. Specifically, semi-analytical methods based on determining linear combinations of detector readings that are least sensitive to changes in the plasma scenario achieve an accuracy of around 5% in fusion power measurements for full-power discharges [17]. Investigations into machine-learning approaches are also ongoing, with techniques based on Principal Component Analysis (PCA) showing comparable performances.

The main concerns with the overall gamma-ray approach to power measurements are twofold: (i) converting fusion gamma-ray emissivities into neutron rates requires accurate knowledge of the gamma-ray-to-neutron branching-ratio for the DT fusion reaction, and (ii) the direct gamma-ray background described in Section 3.3 may paralyse the detectors during high-power discharges, thus limiting the operational range of RGRS.

##### 4.3.1. Branching-ratio

The afore-mentioned GET-ART project has reported a value of  $2.4(5) \times 10^{-5}$  for the gamma-ray-to-neutron branching-ratio. The stated uncertainty, about 21%, does not satisfy the ITER requirements, which include an accuracy no worse than 10% on fusion power measurements. Moreover, the existing literature presents a wide range of results, with values scattered by about a factor of 20 and uncertainties which are inconsistent, suggesting caution. Consequently, dedicated experiments at neutron-sources are planned to determine a reliable value with uncertainty compatible with the ITER requirements. Detailed planning is already underway to conduct measurements at the Monnet fast-neutron source [18] using Time-of-Flight (ToF) techniques.

##### 4.3.2. Operational range

RGRS should provide its (safety-relevant) fusion power measurements for machine protection (MP) purposes. The requirements are: (i) fusion power between 70 and 900 MW, (ii) time resolution of 1 s, and (iii) accuracy no worse than 10%. Given the transport factors calculated for the RGRS detectors, these requirements entail a lower limit on the operational range of 280 kW. Below this value, the integration time necessary to achieve 10% accuracy exceeds the requirements. Therefore, the lower limit of the operational range of RGRS satisfies the requirements.

The situation is more complex for the upper limit, which is determined by the highest count-rate sustainable by the detectors. Based on JET experience, count-rates at the detectors exceeding 500 kHz cannot be compensated for by pile-up recovery techniques [19]. This in turn makes the direct gamma-ray background of Section 3.3 crucial in determining the upper limit for the operational range.

To provide some estimate for this upper limit despite the inherent uncertainty in the direct gamma-ray background, the JET data were used to compute the probability that a neutron interacting with the JET tokamak wall would produce a prompt gamma-ray recorded by the

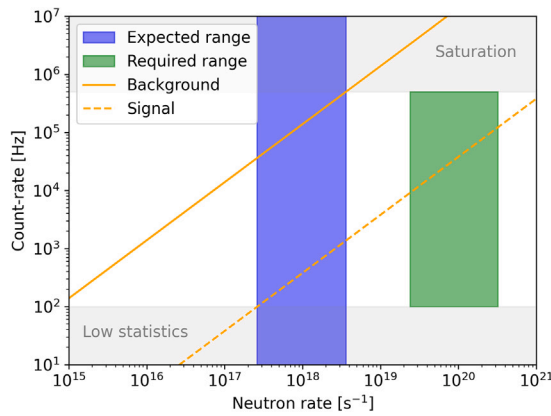


Fig. 5. Operational range of RGRS as found by extrapolating JET results [21].

Table 2

Attenuation performance for various materials. The length of each attenuator was chosen to ensure 10% transmittance at 15 MeV. The background column contains transmittances at 4 MeV, taken as representative background energy.

Material	Length (cm)	Background (%)
C	61.6	1.6
Al	38.8	3.8
Ti	18.5	7.1
Fe	9.4	8.5
W	2.2	17.8

detector [20]. Then, and in spite of the different materials used for first wall and vacuum vessel, this value was used to estimate the background at the ITER detectors given the neutron flux at the LoS footprints.

The resulting operational range, shown in Fig. 5, lies below the power levels required for machine protection. Therefore, it is necessary to shift this range towards higher powers. This can be achieved by placing a gamma-ray attenuator along the LoS, separate from the LiH neutron attenuator. However, most common gamma-attenuating materials - heavy metals - have the disadvantage of preferentially attenuating the signal over the background due to pair-production effects. Consequently, while heavy metals were still investigated, lighter elements were also explored as a potential solution. The results are summarized in Table 2. Not all the examined materials are sensible for adoption due to compatibility issues, such as a too low melting point. However, in view of the substantial uncertainties in the direct gamma-ray background, the final selection of the gamma-ray attenuator is still ongoing.

## 5. Conclusions

The ITER Radial Gamma-Ray Spectrometer (RGRS) is currently undergoing its Preliminary Design Review. The capability of RGRS of satisfying its requirements has not been completely established.

The determination of the  $\alpha$ -particle density profile and energy distribution should exploit  $^{10}\text{B}$  reactions, taking advantage of wall-conditioning. However, the amount of B present in the plasma still has to be quantified in detail. Moreover, the effect of the direct gamma-ray background must be assessed.

The detection of thin-target bremsstrahlung enables RGRS to determine the energy distribution of runaway electrons for currents down to 10 MA in the time-resolved (10 ms) option and 1 MA with a time-integrated (100 ms) measurement. If disruption mitigation through gas injection is adopted, it becomes possible to measure currents as low as 40 kA. The RGRS system is sensitive to the energy distribution of runaway electrons up to 30–40 MeV.

The determination of fusion power with the performance required for Machine Protection is possible provided the gamma-ray-to-neutron

branching-ratio of the DT fusion reaction is known with sufficient accuracy. Dedicated experiments are planned to reduce the uncertainties found in the literature. Moreover, depending on the direct gamma-ray background, which is still to be determined in detail, a gamma-ray attenuator may be needed. Light elements would be especially appropriate to improve the signal-to-noise ratio.

## CRedit authorship contribution statement

**Federico Scioscioli:** Writing – review & editing, Writing – original draft, Methodology, Investigation, Conceptualization. **Giulia Marcer:** Writing – review & editing, Investigation, Formal analysis, Conceptualization. **Alessandro Ciurlino:** Investigation, Formal analysis. **Stefano Colombi:** Investigation. **Bruno Coriton:** Project administration, Investigation. **Andrea Dal Molin:** Investigation. **Jan Dankowski:** Investigation. **Giuseppe Gorini:** Investigation. **Andrei Kovalev:** Supervision, Project administration, Investigation, Formal analysis. **Andrea Muraro:** Investigation. **Massimo Nocente:** Writing – review & editing, Supervision, Investigation, Conceptualization. **Marica Rebai:** Supervision, Investigation. **Davide Rigamonti:** Investigation. **Marco Tardocchi:** Supervision, Investigation. **Gabriele Croci:** Supervision, Investigation, Funding acquisition, Conceptualization.

## Declaration of competing interest

The authors declare that they have no known competing financial interests or personal relationships that could have appeared to influence the work reported in this paper.

## Acknowledgements

The views and opinions expressed herein do not necessarily reflect those of the ITER Organization.

## Data availability

Data will be made available on request.

## References

- [1] M. Nocente, A.D. Molin, N. Eidiētis, L. Giacomelli, G. Gorini, Y. Kazakov, E. Khilkevitch, V. Kiptily, M. Iliasova, A. Lvovskiy, M. Mantsinen, A. Mariani, E. Panontin, G. Papp, G. Pautasso, C. Paz-Soldan, D. Rigamonti, M. Salewski, A. Shevelev, M. Tardocchi, JET, MST1, contributors, MeV range particle physics studies in tokamak plasmas using gamma-ray spectroscopy, *Plasma Phys. Control. Fusion* 62 (1) (2019) <http://dx.doi.org/10.1088/1361-6587/ab4f32>.
- [2] V. Kiptily, A.E. Shevelev, V. Goloborod'ko, M. Kocan, E. Veshchev, T. Craciunescu, E. Khilkevitch, I. Lengar, I.A. Polunovsky, K. Schoepf, S.M. Soare, V. Yavorskij, V. Zaita, Escaping alpha-particle monitor for burning plasmas, *Nucl. Fusion* 58 (2018).
- [3] M. Nocente, A. Shevelev, L. Giacomelli, G. Pautasso, M. Tardocchi, D. Gin, M. Gobbin, G. Gorini, A. Fernandes, A. Herrmann, E. Khilkevitch, E. Panontin, G. Papp, R.C. Pereira, M. Salewski, G. Tardini, M. Valisa, A.U. Team, E.M. Team, High resolution gamma-ray spectrometer with MHz capabilities for runaway electron studies at ASDEX upgrade, *Rev. Sci. Instrum.* 89 (10) (2018) 101124, <http://dx.doi.org/10.1063/1.5036658>.
- [4] A.D. Molin, M. Nocente, M.D. Rosa, E. Panontin, D. Rigamonti, M. Tardocchi, A. Shevelev, E. Khilkevitch, M. Iliasova, L. Giacomelli, G. Gorini, E.P. Cippo, F. D'Isa, G. Pautasso, G. Papp, G. Tardini, E. Macusova, J. Cerovsky, O. Ficker, M. Salewski, V. Kiptily, the EUROfusion MST1 Team, the COMPASS Team, the ASDEX Upgrade Team, A new hard x-ray spectrometer for runaway electron measurements in tokamaks, *Meas. Sci. Technol.* 34 (8) (2023) <http://dx.doi.org/10.1088/1361-6501/acd46c>.
- [5] M. Rebai, D. Rigamonti, A. Dal Molin, G. Marcer, A. Bracco, F. Camera, D. Farina, G. Gorini, E. Khilkevitch, M. Nocente, E. Perelli Cippo, O. Putignano, J. Scionti, A. Shevelev, A. Zohar, M. Tardocchi, First direct measurement of the spectrum emitted by the  $^3\text{H}(^2\text{H},\gamma)^4\text{He}$  reaction and assessment of the relative yield  $\gamma_1$  to  $\gamma_0$ , *Phys. Rev. C* 110 (2024) 014625, <http://dx.doi.org/10.1103/PhysRevC.110.014625>.

- [6] A. Dal Molin, G. Marcer, M. Nocente, M. Rebai, D. Rigamonti, M. Angelone, A. Bracco, F. Camera, C. Cazzaniga, T. Craciunescu, G. Croci, M. Dalla Rosa, L. Giacomelli, G. Gorini, Y. Kazakov, E.M. Khilkevitch, A. Muraro, E. Panontin, E. Perelli Cippo, M. Pillon, O. Putignano, J. Scionti, A.E. Shevelev, A. Žohar, M. Tardocchi, Measurement of the Gamma-ray-to-neutron branching ratio for the deuterium-tritium reaction in magnetic confinement fusion plasmas, *Phys. Rev. Lett.* 133 (2024).
- [7] B. Esposito, D. Marocco, G. Gandolfo, F. Belli, L. Bertalot, J. Blocki, D. Bocian, G. Brolatti, M. Ceconello, C. Centioli, R. Costa Pereira, S. Conroy, F. Crescenzi, N. Cruz, L. Bilbao, A. Domenicone, Q. Ducasse, G. Di Mambro, D. Dongiovanni, A. Zimbal, Progress of design and development for the ITER radial neutron camera, *J. Fusion Energy* 41 (2022) <http://dx.doi.org/10.1007/s10894-022-00333-9>.
- [8] M. Scholz, A. Hjalmarsson, L. Hajduk, G. Ericsson, J. Kotula, U. Woźnicka, J. Blocki, B. Brichard, S. Conroy, K. Drozdowicz, L. Giacomelli, J. Godlewski, C. Hellesen, A. Igielski, R. Kantor, A. Kurowski, B. Marcinkevicius, G. Mazzone, M. Mrzyglod, A. Wójcik, Conceptual design of the high resolution neutron spectrometer (HRNS) for ITER, *Nucl. Fusion* 59 (2019) <http://dx.doi.org/10.1088/1741-4326/ab0dc1>.
- [9] Alloy Digest, HIPERCO 50A: Soft magnetic alloy, 1999, <http://dx.doi.org/10.31399/asm.ad.co0107>.
- [10] C. Cazzaniga, M. Nocente, M. Tardocchi, M. Rebai, M. Pillon, F. Camera, A. Giaz, L. Pellegrini, G. Gorini, Response of LaBr<sub>3</sub>(Ce) scintillators to 14MeV fusion neutrons, *Nucl. Instrum. Methods Phys. Res. Sect. Accel. Spectrom. Detect. Assoc. Equip.* 778 (2015) 20–25, <http://dx.doi.org/10.1016/j.nima.2015.01.002>.
- [11] M. Curuia, T. Craciunescu, S. Soare, V. Zoita, V. Braic, D. Croft, A. Fernandes, J. Figueiredo, V. Goloborod'ko, G. Gorini, S. Griph, V. Kiptily, I. Lengar, S. Mianowski, J. Naish, R. Naish, M. Nocente, R.C. Pereira, V. Riccardo, K. Schoepf, B. Santos, M. Tardocchi, V. Yavorskij, I. Zychor, Upgrade of the tangential gamma-ray spectrometer beam-line for JET DT experiments, *Fusion Eng. Des.* 123 (2017) 749–753, <http://dx.doi.org/10.1016/j.fusengdes.2017.05.064>, Proceedings of the 29th Symposium on Fusion Technology (SOFT-29) Prague, Czech Republic, September 5-9, 2016.
- [12] M. Nocente, V. Kiptily, M. Tardocchi, P.J. Bonofiglio, T. Craciunescu, A.D. Molin, E. De La Luna, J. Eriksson, J. Garcia, Z. Ghani, G. Gorini, L. Hägg, Y. Kazakov, E. Lerche, C.F. Maggi, P. Mantica, G. Marcer, M. Maslov, O. Putignano, D. Rigamonti, M. Salewski, S. Sharapov, P. Siren, Z. Stancar, A. Zohar, P. Beaumont, K. Crombe, G. Ericsson, M. Garcia-Munoz, D. Keeling, D. King, K. Kirov, M.F.F. Nave, J. Ongena, A. Patel, C. Perez von Thun, J. Contributors, Fusion product measurements by nuclear diagnostics in the joint European Torus deuterium-tritium 2 campaign (invited), *Rev. Sci. Instrum.* 93 (9) (2022) 093520, <http://dx.doi.org/10.1063/5.0101767>.
- [13] V. Afanasyev, F. Chernyshev, S. Kozlovsky, A. Melnik, G. Marinin, M. Mironov, A. Navolotsky, V. Nesenevich, M. Petrov, S. Petrov, A. Yatsenko, I. Chugunov, D. Doinikov, M. Iliasova, D. Gin, E. Khilkevitch, I. Polunovsky, A. Shevelev, K. Artemev, V. Krasilnikov, T. Kormilitsyn, A. Kovalev, A. Mokeev, M. Turnyanskiy, Development of the NPA based diagnostic complex in ITER, *J. Instrum.* 17 (07) (2022) C07001, <http://dx.doi.org/10.1088/1748-0221/17/07/C07001>.
- [14] SWX-277 high temperature shielding technical information, 2024, <https://www.shieldwrx.com/castable-shielding>. (Accessed 31 October 2024).
- [15] C. Angioni, Impurity transport in tokamak plasmas, theory, modelling and comparison with experiments, *Plasma Phys. Control. Fusion* 63 (7) (2021) 073001, <http://dx.doi.org/10.1088/1361-6587/abfc9a>.
- [16] M. Nocente, M. Tardocchi, R. Barnsley, L. Bertalot, B. Brichard, G. Croci, G. Brolatti, L. Pace, A. Fernandes, L. Giacomelli, I. Lengar, M. Moszynski, A. Krasilnikov, A. Muraro, R. Costa Pereira, E. Cippo, D. Rigamonti, M. Rebai, J. Rzdakiewicz, M. Salewski, P. Santosh, J. Sousa, I. Zychor, G. Gorini, Conceptual design of the Radial Gamma Ray Spectrometers system for  $\alpha$  particle and runaway electron measurements at ITER, *Nucl. Fusion* 57 (2017).
- [17] G. Marcer, F. Scioscioli, G. Croci, A. Dal Molin, G. Gorini, A. Muraro, M. Nocente, E. Perelli Cippo, M. Rebai, D. Rigamonti, B. Coriton, A. Kovalev, A. Polevoi, E. Khilkevitch, A. Shevelev, A. Bracco, F. Camera, C. Cazzaniga, M. Tardocchi, Development of a measuring technique based on JET second D-T campaign (DTE2) experience for assessing fusion power at ITER during D-T operation using the radial gamma-ray spectrometer, *Rev. Sci. Instrum.* 95 (8) (2024) 083515, <http://dx.doi.org/10.1063/5.0217677>.
- [18] C. Fontana, B. Cédric, W. Geerts, M. Martinez, M. Vidali, S. Oberstedt, JRC MONNET – the intense fast-neutron source for fundamental and application-driven research, *EPJ Web Conf.* 284 (2023) <http://dx.doi.org/10.1051/epjconf/202328406002>.
- [19] G. Marcer, A. Dal Molin, M. Rebai, D. Rigamonti, M. Tardocchi, Degenerate pile-up correction in pulse height spectra from Gamma-ray spectrometers, *J. Fusion Energy* 43 (1) (2024) <http://dx.doi.org/10.1007/s10894-024-00409-8>.
- [20] S.L. Fugazza, G. Marcer, M. Nocente, A. Ciurlino, G. Croci, M.D. Rosa, A.D. Molin, E. Gallo, G. Gorini, M. Parisi, P. Raj, M. Rebai, M. Reinke, D. Rigamonti, F. Scioscioli, M. Tardocchi, First scoping study of a gamma-ray detector for fusion power measurements at the SPARC tokamak, *Fusion Eng. Des.* (2025) for publication.
- [21] G. Marcer, A Novel Method for DT Fusion Power Measurement in Magnetic Confinement Plasmas Based on the Gamma Ray Emission from The D(T,<sup>3</sup>He)<sub>γ</sub> Reaction (Ph.D. thesis), University of Milano-Bicocca, 2025.